

## Si 2*p* and 2*s* resonant excitation and photoionization in SiF<sub>4</sub>

T. A. Ferrett,\* M. N. Piancastelli,† D. W. Lindle,\* P. A. Heimann,‡ and D. A. Shirley

*Department of Chemistry, University of California, Berkeley, California 94720*

*and Materials and Chemical Sciences Division, Lawrence Berkeley Laboratory, 1 Cyclotron Road, Berkeley, California 94720*

(Received 14 December 1987)

We present partial-cross-section results for Si 2*p* and valence photoionization of SiF<sub>4</sub> for photon energies in the vicinity of the Si 2*p* and 2*s* thresholds. The continuum shape resonances decay only to the Si 2*p* main line, in accordance with one-electron theory predictions. The Si *L*<sub>2,3</sub>*VV* Auger spectrum was also measured, and was found to agree with earlier work. We propose that variations in hole-interaction energies are important in assigning the Auger final states. For the Si 2*p* discrete excitations, spectra obtained on the  $\sigma^*(a_1)$  resonances compare well with previous qualitative results and the above-threshold Si *L*<sub>2,3</sub>*VV* Auger spectrum. Our results help to quantify the relative enhancement of satellites and main lines, emphasizing the dominance of spectator decay. Spectra obtained at several higher-energy Si 2*p* and Si 2*s* excitations also generally support spectator decay as an important mode of relaxation for these discrete states. The overall assignment of the Si 2*p* and 2*s* discrete excitations to molecular-orbital and Rydberg transitions is discussed.

### I. INTRODUCTION

Core-level absorption spectra of a series of S- and Si-containing molecules have been interpreted using a potential-barrier model to explain intense features in terms of transitions to unoccupied molecular orbitals.<sup>1-4</sup> In this model, the centrifugal barrier can trap an outgoing photoelectron, which then tunnels through the barrier and emerges in the continuum with enhanced intensity.<sup>5</sup> In particular, the excitation spectra of the series including SO<sub>2</sub>, SiF<sub>4</sub>, and SF<sub>6</sub> illustrate that the continuum resonances are more pronounced for molecules of high symmetry which contain electronegative ligands; these factors seem to enhance the barrier both directionally and in terms of repulsion from electronegative atoms. The narrowest and most intense resonances are found above the S 2*p* subshell threshold of SF<sub>6</sub>, whereas the corresponding SO<sub>2</sub> absorption spectrum exhibits much broader and weaker continuum features.<sup>6,7</sup> Furthermore, photoemission experiments on the S 2*p* main-line ionization of SF<sub>6</sub> have demonstrated that the feature assigned as the *e<sub>g</sub>* shape resonance exhibits strong electron-correlation effects through coupling to a neighboring S 2*p* shake-up satellite.<sup>8</sup> For the discrete portions of these *L*<sub>2,3</sub> spectra, SF<sub>6</sub> and SO<sub>2</sub> also show two extreme forms of behavior. The SF<sub>6</sub> oscillator strength appears primarily in S 2*p* excitations to molecular orbitals, while both molecular-orbital and Rydberg transitions dominate the spectrum of SO<sub>2</sub> below the S 2*p* edge.

Between these two extremes falls the intermediate case of SiF<sub>4</sub>,<sup>7,9</sup> which has two continuum resonances above the Si 2*p* edge, first proposed to be shape resonances of *e* and *t*<sub>2</sub> symmetry,<sup>2</sup> in addition to a number of discrete excitations below the Si 2*p* threshold (see Fig. 1). The shape resonances have been studied both experimentally<sup>10</sup> and theoretically<sup>10,11</sup> in valence photoionization of SiF<sub>4</sub>, where a number of resonances of *a*<sub>1</sub>, *e*, and *t*<sub>2</sub> symmetry are present. For core ionization, the Si 2*p* asymmetry pa-

rameter  $\beta$  has been measured previously,<sup>12</sup> and some partial cross-section results were reported recently for the Si 2*p* level,<sup>13</sup> in disagreement with photoabsorption data<sup>9</sup> at the first shape resonance ( $\sim 117$  eV).

The discrete portion of the Si 2*p* absorption spectrum of SiF<sub>4</sub> was initially explained solely by invoking Rydberg transitions.<sup>14</sup> Later assignments,<sup>9,15</sup> supported by the

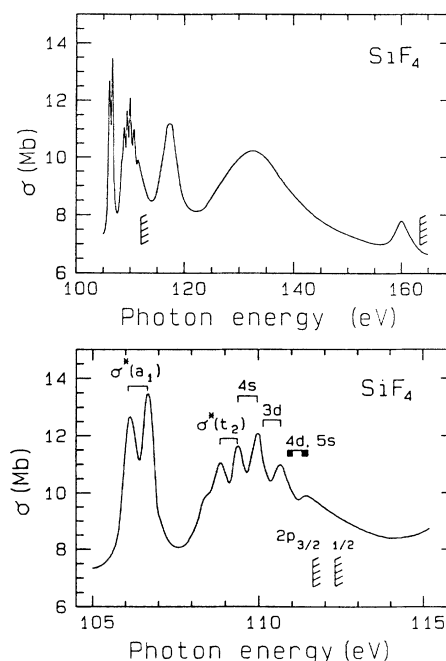


FIG. 1. Total photoabsorption cross section (Ref. 9) of gaseous SiF<sub>4</sub>. The top panel shows the extended energy-range spectrum including the Si 2*p* shape resonances at 117 and 133 eV photon energy and the Si 2*s* excitations near 160 eV. The discrete features in the expanded spectrum in the bottom panel have been interpreted (Ref. 9) as overlapping molecular and Rydberg excitations, as labeled.

analogous experiment on solid SiF<sub>4</sub>, postulated overlapping molecular-orbital and Rydberg excitations. Finally, absorption experiments on Si 1s ionization of SiF<sub>4</sub> suggest that distortion of the excited state to a trigonal bipyramid may be necessary to explain the complexity of all the core-level discrete spectra.<sup>16</sup>

We present here further photoelectron spectroscopic measurements of the Si 2*p* and valence photoionization cross sections in the vicinity of the Si 2*p* and 2*s* thresholds of SiF<sub>4</sub>. This study has been performed with both improved sensitivity and resolution relative to earlier work. Our Si 2*p* partial cross section does display the prominent resonance at 117 eV in photoabsorption,<sup>9</sup> in disagreement with earlier results.<sup>13</sup> The above-threshold Si L<sub>2,3</sub>VV Auger spectrum was also observed, and the kinetic energies and relative intensities compare well with those of Aksela *et al.*<sup>17</sup> We discuss the assignment of Rye and Houston<sup>18</sup> for the Auger final states and an alternate model which accounts for variations in hole-hole interactions for the various configurations. We have made the first quantitative study of the decay channels of the discrete Si 2*p* and 2*s* excitations, and in some cases have assigned the resonant spectra qualitatively by comparison to the Si L<sub>2,3</sub>VV Auger spectrum.

The experimental details are presented in Sec. II. Section III includes the Si 2*p* continuum results and the Si L<sub>2,3</sub>VV Auger spectrum. We present the discrete resonant results for Si 2*p* excitation in Sec. IV, and for Si 2*s* excitation in Sec. V. Conclusions appear in Sec. VI.

## II. EXPERIMENTAL

The experiment was performed at the Stanford Synchrotron Radiation Laboratory (SSRL) on the Beam line III-1 "grasshopper" monochromator using a 1200-line/mm holographically ruled grating. The experimental apparatus and methods have been described previously.<sup>19–21</sup> Briefly, a time-of-flight (TOF) electron analyzer situated at the "magic angle" of 54.7° relative to the photon polarization direction allows measurement of angle-independent partial cross sections, based on Yang's theorem.<sup>22</sup> The analyzer transmission as a function of kinetic energy was calibrated with the known partial cross sections for Ne<sup>+</sup>(2*s*) and Ne<sup>+</sup>(2*p*) photoelectrons.<sup>23</sup>

A 1000-Å-thick silicon window separated the monochromator (10<sup>-9</sup> torr) from the gas chamber (10<sup>-5</sup> torr). The gas pressure was monitored behind the effusive nozzle with a capacitance manometer. The relative photon flux was calibrated by detecting fluorescence from sodium salicylate with a phototube (RCA 8850). Corrections for the varying response of sodium salicylate with photon energy have been applied to the partial cross-section results.<sup>24</sup> Statistical errors only are shown in our plots. We estimate that systematic errors for the nonresonant cross sections are ±10%, and for the resonant results ±3%.

The monochromator bandpass for the Si 2*p* and Si 2*s* continua studies varied from 0.65–1.40 eV FWHM (full width at half maximum) (a constant 0.66 Å) over the photon-energy range 110–165 eV. For the resonances below the Si 2*p* threshold, a bandpass of 0.25 eV (0.26 Å)

was used. Energy calibration to within 0.20 eV was obtained over the range of the experiment from the resonance positions in the SiF<sub>4</sub> photoabsorption spectrum.<sup>9</sup> For reference, the binding energies of the valence and core levels in SiF<sub>4</sub> are set out in Table I.

## III. THE Si 2*p* CONTINUUM

In Sec. III A we present the partial cross sections for the inner- and outer-valence peaks and for the Si 2*p* main line in the photon-energy range 114–165 eV, where two intense continuum resonances are present.<sup>2,3,9</sup> These results are compared with other experimental measurements<sup>13</sup> and with multiple-scattering (MS) *Xα* theory<sup>2,3,13</sup> in an attempt to identify the symmetry of the shape resonances. We present the Si L<sub>2,3</sub>VV Auger spectrum in Sec. III B. A previous interpretation and assignment<sup>18</sup> of the Auger peaks with respect to hole localization is discussed.

### A. Partial cross sections

A TOF spectrum in Fig. 2 illustrates the outer- and inner-valence groups, the Si L<sub>2,3</sub>VV Auger peaks, and the Si 2*p* main line. To investigate the intensity variations over the resonances at 117 and 133 eV photon energy observed in photoabsorption<sup>2,3,9</sup> we have measured the relative partial cross sections for valence and Si 2*p* ionization. Figure 3 shows these data.

We compare our Si 2*p* results to those of Bancroft *et al.*<sup>13</sup> in the top panel of Fig. 3, where our relative cross sections have been scaled at  $h\nu=136$  eV. When the data are scaled in this manner for agreement at the second resonance ( $h\nu=133$  eV), there is significant disagreement below  $h\nu=120$  eV where the resonant effect is more pronounced in our data. We have no explanation this difference. Bancroft *et al.*<sup>13</sup> noted that their Si 2*p* results at this resonance were lower than the photoabsorption

TABLE I. Binding energies of the pertinent molecular valence and core levels in SiF<sub>4</sub>.

Orbital	Binding energy (eV)
Outer valence <sup>a</sup>	
1 <i>t</i> <sub>1</sub>	16.4
5 <i>t</i> <sub>2</sub>	17.5
1 <i>e</i>	18.1
4 <i>t</i> <sub>2</sub>	19.5
5 <i>a</i> <sub>1</sub>	21.5
Inner valence <sup>b</sup>	
3 <i>t</i> <sub>2</sub>	39.3
4 <i>a</i> <sub>1</sub>	40.6
Si 2 <i>p</i> (2 <i>t</i> <sub>2</sub> ) <sup>c</sup>	111.6
Si 2 <i>s</i> (3 <i>a</i> <sub>1</sub> ) <sup>d</sup>	163.6

<sup>a</sup>Reference 33.

<sup>c</sup>Reference 17.

<sup>b</sup>Reference 34.

<sup>d</sup>Reference 16.

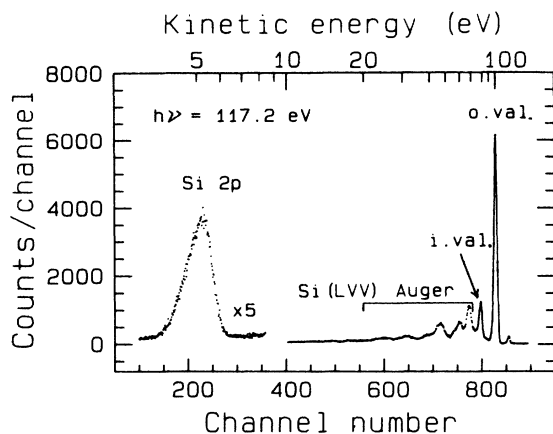


FIG. 2. TOF photoelectron spectrum of  $\text{SiF}_4$  taken at  $\theta=54.7^\circ$  and  $h\nu=117.2$  eV, at the peak of the first Si 2p continuum resonance. The outer- and inner-valence peaks are labeled o. val and i. val, respectively. The Si  $L_{2,3}VV$  Auger peaks appear at somewhat lower kinetic energy.

curves<sup>2,3,9</sup> would indicate, and ascribed the difference to possible contributions from shake-up, shake-off, and photodissociation. Because our results are more in line with the relative intensities in photoabsorption, we believe that other processes as mentioned above are probably less significant in this energy region than at the second resonance. Energy arguments alone suggest that at 5 eV

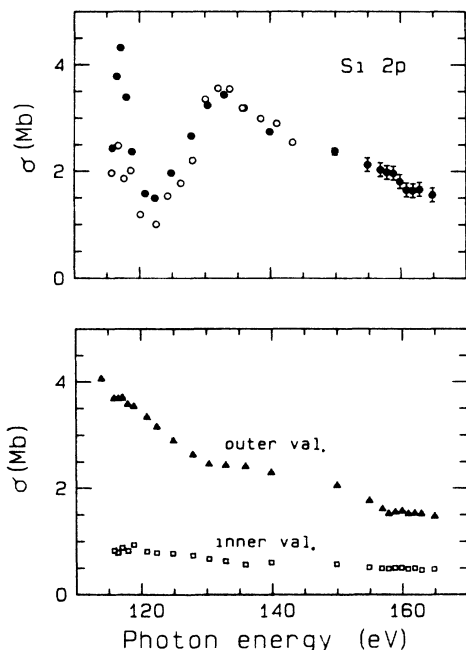


FIG. 3. Top panel: partial cross sections for Si 2p photoionization (closed circles), compared with the results of Bancroft *et al.*<sup>13</sup> (open circles). Our relative cross sections have been scaled to the absolute values of Bancroft *et al.* at  $h\nu=136$  eV. Bottom panel: summed outer-valence (closed triangles) and inner-valence (open squares) partial cross sections were determined using the scaling of the Si 2p values. In both panels, statistical error bars are either shown or are smaller than the symbol size.

above the Si 2p threshold, shake-up and shake-off processes involving a Si 2p electron should be negligible.

For the valence ionization cross sections (Fig. 3, bottom) there is no evidence of enhancement at either continuum resonance, in agreement with the observations of Bancroft *et al.*<sup>13</sup> Our inner-valence cross section agrees well with other reported values,<sup>13</sup> and is systematically lower than MS  $X\alpha$  calculations<sup>13</sup> by about a factor of 2. There are as yet no experimental or theoretical results available for comparison to our outer-valence results in this energy range.

The lack of valence enhancement at the Si 2p continuum resonances is also seen for the S 2p ionization in  $\text{SF}_6$ .<sup>8</sup> However, for  $\text{SF}_6$  a S 2p satellite was found to be resonant at the second continuum resonance ( $e_g$ ), suggesting that a many-electron treatment of this  $e_g$  shape resonance is necessary. For  $\text{SiF}_4$  we see no Si 2p satellite enhancement at either continuum resonance. Thus the qualitative behavior of the Si 2p shape resonances is well modeled in a one-electron description,<sup>1,5</sup> with decay only to the Si 2p main line.

The assignment of the Si 2p continuum resonances in  $\text{SiF}_4$  has been discussed by several workers. There is uniform agreement that the feature at  $\sim 22$  eV kinetic energy ( $h\nu=133$  eV) is a shape resonance of  $t_2$  symmetry. This is supported by early MS  $X\alpha$  theory<sup>2,3</sup> and more recent calculations by Bancroft *et al.*<sup>13</sup> Furthermore, this resonance is seen in experiment and theory for several valence levels of  $\text{SiF}_4$ .<sup>10</sup> However, the symmetry of the resonance at  $\sim 5$  eV kinetic energy ( $h\nu=117$  eV) is much less definite. Early MS  $X\alpha$  calculations found shape resonances of  $e$  symmetry at  $\sim 4$ – $6$  eV and  $13$ – $15$  eV,<sup>2,3</sup> whereas later results<sup>13</sup> found an  $e$  resonance at 14 eV, an  $a_1$  resonance at 3.3 eV, and a weak  $t_2$  feature at 6.8 eV kinetic energy. Bancroft *et al.*<sup>13</sup> eventually assigned the intense 5-eV resonance as  $t_2$  despite the very weak presence of this feature in theory. Bancroft *et al.*<sup>13</sup> also have used experimental and theoretical results on  $\text{SiCl}_4$  (where the agreement is less ambiguous<sup>2,25</sup>) by analogy to support the  $t_2$  assignment for the 5-eV resonance. We note that part of this explanation involved assignment of a resonance of  $e$  symmetry in  $\text{SiF}_4$  (as found in theory in moderate intensity<sup>13</sup>) at about 10 eV kinetic energy. A very small shoulder at this energy is evident in one photoabsorption spectrum,<sup>2</sup> but not in a later measurement.<sup>9</sup> We do not discern a resonance in our data near 10 eV.

Because of the lack of agreement among various theoretical calculations, we believe it is not possible at this time to identify the 5-eV resonance ( $h\nu=117$  eV) definitely as having either  $e$  or  $t_2$  symmetry. It is unlikely that further experimental results alone will help clarify this situation. Theory, which has produced widely varying results for  $\text{SiF}_4$ , is clearly sensitive to the details of the calculations. This model-dependent sensitivity needs to be resolved before the theory can be used with confidence.

#### B. Si $L_{2,3}VV$ Auger spectrum

Rye and Houston<sup>18</sup> obtained the first Si  $L_{2,3}VV$  Auger spectrum for  $\text{SiF}_4$  using electron-beam impact. Scattered

electrons created a steeply sloping background, making the derivation of Auger intensities difficult. More recently, Aksela *et al.*<sup>17</sup> observed the Auger spectrum using synchrotron radiation. We will compare our quantitative results to those of Aksela *et al.*<sup>17</sup> and discuss the peak assignments originally proposed by Rye and Houston.<sup>18</sup>

Our Si  $L_{2,3}VV$  Auger spectrum is plotted in the top of Fig. 4 as a function of kinetic energy. Peak labels *a* through *f* follow the notation of Aksela *et al.*<sup>17</sup> and are reversed from the notation of Rye and Houston.<sup>18</sup> In Table II we include the peak kinetic energies and relative intensities compared with those of Aksela *et al.*<sup>17</sup> The kinetic energies are in agreement within error limits, and the relative intensities are quite similar. There is a small discrepancy for peaks *d* and *e*. We find peak *d* to be slightly more intense than peak *e*; the reverse is true for the data of Ref. 17.

The Auger peak assignments proposed by Rye and Houston<sup>18</sup> involve first an assumption that only valence orbitals with appreciable Si character in neutral  $\text{SiF}_4$  will participate in the decay. This rules out the outermost three orbitals ( $1t_1$ ,  $5t_2$ , and  $1e$ ) which are essentially *F* lone pairs. In this approach, the remaining valence orbitals ( $4t_2$ ,  $5a_1$ ,  $3t_2$ , and  $4a_1$ ) combine to give the following generic Auger final states in terms of outer- and inner-valence holes (see Table I): (i) two outer-valence holes, (ii) one inner-valence hole and one outer-valence hole, (iii) two inner-valence holes. With a constant hole-hole repulsion energy assumed for all final states and the observation that the inner- and outer-valence binding energies within each group are closely spaced, this provides for three distinct groups of peaks in the Auger spectrum, whereas six peaks are observed. Rye and Houston explained this apparent “doubling” by postulating that the two valence holes in a single configurational final state appear spatially in the same Si—F bond or in different bonds.<sup>18</sup>

While this model has the valuable feature of addressing hole-hole repulsion, spatial localization on specific bonds seems less likely for valence-shell holes than delocalization in molecular orbitals. An alternate description of the  $\text{SiF}_4^{+2}$  Auger final states extends the idea of hole localization. Each of the two-hole final states may be described by coupling two one-hole states, which are in turn given by delocalized molecular orbitals. This model has the advantage that the molecular orbitals transform as

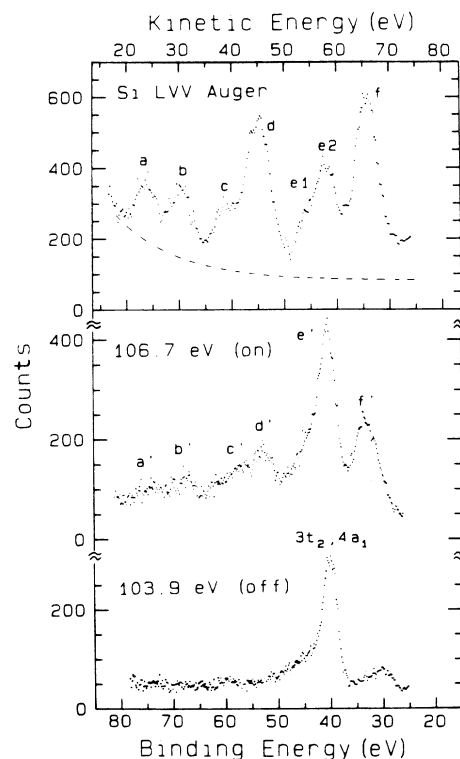


FIG. 4. Comparison of the Si  $L_{2,3}VV$  Auger spectrum (top panel) with the resonant satellite spectrum taken at  $h\nu=106.7$  eV at the  $\sigma^*(a_1)$  discrete excitation. A nonresonant spectrum taken at  $h\nu=103.9$  eV is shown in the bottom panel, where only the inner-valence main lines ( $3t_2, 4a_1$ ) and some small satellites are present. The Auger spectrum is labeled as in Ref. 17. Note that the kinetic energy scale at the top applies only to the Auger spectrum. We do not show the outer-valence region here, in which there was very little resonant enhancement (see Fig. 6). The nearly direct correspondence between the Auger and resonant spectra implies the presence of spectator satellites in the resonant spectrum with the same two-hole configurations as in the Auger spectrum, plus the initially excited electron [ $\sigma^*(a_1)$ ].

the symmetry group of the molecule, and thus simulate eigenstates of the  $\text{SiF}_4^{+2}$  Hamiltonian. In coupling the two one-hole states, due account must of course be taken of hole-hole repulsion as well as of electron polarization toward the holes. Like Rye and Houston,<sup>18</sup> we assume that  $\text{SiF}_4^+$  and  $\text{SiF}_4^{+2}$  remain essentially intact during

TABLE II. Si  $L_{2,3}VV$  Auger peak energies and relative intensities for  $\text{SiF}_4$ .

Auger peak label (Ref. 17)	Kinetic energy (eV)		Relative intensity (%)	
	Present	Ref. 17	Present <sup>a</sup>	Ref. 17
<i>a</i>	24.3(4)	23.7(5)	5.8	5.7
<i>b</i>	30.8(3)	30.7(3)	8.7	7.0
<i>c</i>	39.4(5)	39.6(3)	7.5	7.3
<i>d</i>	45.3(8)	45.4(2)	25.0	21.7
<i>e</i> <sub>1</sub>	54.4(10)	55.2(3)	20.6 <sup>b</sup>	8.1
<i>e</i> <sub>2</sub>	58.2(8)	58.7(3)		16.3
<i>f</i>	66.1(5)	66.3(2)	32.5	33.9

<sup>a</sup>Uncertainty is  $\pm 1\%$ .

<sup>b</sup>For the summed intensity of peaks *e*<sub>1</sub> and *e*<sub>2</sub>.

the photoionization and Auger processes. To first order, we start with the same three peak groupings above, as per Rye and Houston:<sup>18</sup> (i) two outer-valence holes:

$$(4t_2)^{-2}, (5a_1)^{-2}, (4t_2)^{-1}(5a_1)^{-1},$$

(ii) one outer-valence hole and one inner-valence hole:

$$(4t_2)^{-1}(3t_2)^{-1}, (4t_2)^{-1}(4a_1)^{-1},$$

$$(5a_1)^{-1}(3t_2)^{-1}, (5a_1)^{-1}(4a_1)^{-1},$$

(iii) two inner-valence holes:

$$(3t_2)^{-2}, (4a_1)^{-2}, (4a_1)^{-1}(3t_2)^{-1}.$$

We propose that the energies of individual configurations are shifted by different amounts depending on the hole-hole interactions. Support for this approach comes from recent calculations for the energies of Auger two-hole final states of  $N_2O^{+2}$ , which indicate differences of nearly 6 eV in the magnitude of the hole interaction energies.<sup>26</sup> Considering also the various ways to couple two holes in the final state, a more accurate determination of the hole interaction energies may introduce more complexity into the  $SiF_4$  Si  $L_{2,3}VV$  Auger spectrum. Because of this complexity, and the partially resolved lines shown in Fig. 4, we shall not attempt to give explicit spectral assignments. We note that preliminary calculations, similar to those on  $N_2O^{+2}$ , do find significant differences in the hole-interaction energies, though not completely explaining the observed spectrum.<sup>27</sup> Thus a final assignment of the Auger spectrum may require inclusion of other effects.

#### IV. DISCRETE RESONANCES BELOW THE Si 2p THRESHOLD

Figure 1 (bottom) illustrates the discrete resonances below the Si 2p edge, including a particular assignment based on the overlap of molecular orbital and Rydberg excitations.<sup>9</sup> We have studied the decay channels to  $SiF_4^+$  in the vicinity of the resonances at 106.1 and 106.7 eV, assigned as the molecular-orbital excitations Si

$2p_{3/2,1/2} \rightarrow \sigma^*(a_1)$ .<sup>9</sup> Using the Si  $L_{2,3}VV$  Auger spectrum for comparison, in Sec. IV A we interpret the resonance photoemission spectra and present partial cross sections for the valence main lines and some of the resonantly enhanced valence satellites. We discuss the qualitative aspects of the decay at the different resonances in Sec. IV B, where we present a few spectra taken in the vicinity of the higher resonances in the range  $h\nu=108-112$  eV.

##### A. The Si 2p $\rightarrow \sigma^*(a_1)$ resonance

In Fig. 4 we show a nonresonant photoelectron spectrum at  $h\nu=103.9$  eV which includes the unresolved inner-valence main lines ( $3t_2$  and  $4a_1$ ) and some valence satellites at 30 eV binding energy. The inner-valence peak shows some intensity on the high binding-energy side, also observed by Aksela *et al.*<sup>17</sup>

On resonance, at  $h\nu=106.7$  eV, we see enhancement of a number of valence satellites (Fig. 4). The spectra in Fig. 4, as plotted, are uncorrected for analyzer transmission, which decreases by a factor of 2 from right to left over the energy range of the bottom two spectra in Fig. 4. Partial cross sections reported here have been corrected for transmission.

To aid in interpretation of the resonant spectra, we have aligned the Si  $L_{2,3}VV$  Auger spectrum, excited above the Si 2p threshold at  $h\nu=117.2$  eV, with the  $h\nu=106.5$ -eV resonance spectrum in Fig. 4 for comparison. Although the intensities are somewhat different, the same peak pattern appears in both spectra. Table III lists the binding energies of the resonantly enhanced valence satellites and relates each satellite to the corresponding Auger peak on resonance. There is a one-to-one correspondence to the Auger peaks *a* through *f* with the minor exception of peak *e*, where the resonance spectrum shows only a single broad peak. This similarity is consistent with each peak in the resonance spectrum arising from a two-hole state (plus an excited electron).

To help illustrate the close relationship between the resonantly enhanced valence satellites and the corre-

TABLE III.  $SiF_4$  valence satellites resonant at the  $Si(2p) \rightarrow \sigma^*(a_1)$ ,  $\sigma^*(t_2)$ , and Rydberg excitations.

Photon energy (eV)	Resonance assignment (Ref. 9)	Satellite binding energy (eV)	Corresponding <sup>a</sup> Auger peak and kinetic energy (eV)
106.1	Si $2p_{3/2} \rightarrow \sigma^*(a_1)$	33(1)	<i>f</i> : 66.1
106.7	Si $2p_{1/2} \rightarrow \sigma^*(a_1)$	[40(1)] <sup>b</sup>	<i>e</i> <sub>1</sub> , <i>e</i> <sub>2</sub> : 54.4, 58.2
		53(1)	<i>d</i> : 45.3
		57(1)	<i>c</i> : 39.4
		68(1)	<i>b</i> : 30.8
		74(1)	<i>a</i> : 24.3
108.8	Si $2p_{3/2} \rightarrow \sigma^*(t_2)$	37(1)	
110.6	Si $2p \rightarrow 3d, 4d, 5s$ Rydberg	44(1)	

<sup>a</sup>A direct spectral comparison is made in Fig. 4. Peak energies from our results, Table II.

<sup>b</sup>Although this peak is approximately at the binding energy for the inner-valence main lines, comparison with peaks *e*<sub>1</sub> and *e*<sub>2</sub> in the Si  $L_{2,3}VV$  Auger spectrum suggests the presence of a satellite state at this energy also. Mixing of these single-hole (main lines) and two-hole states (satellites) will complicate the peak assignments.

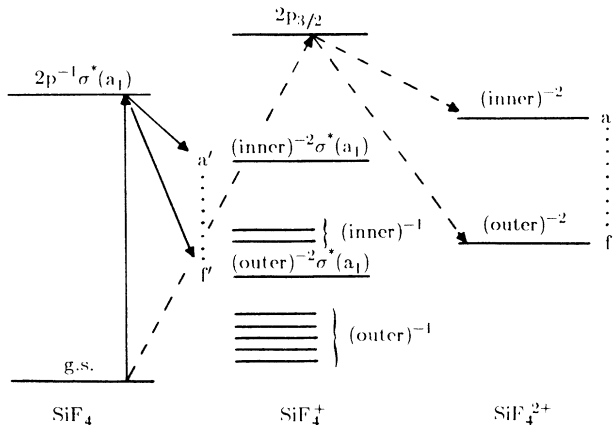


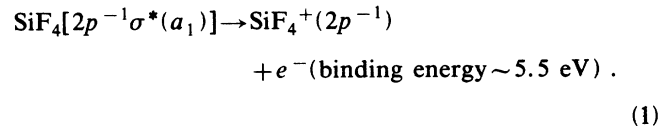
FIG. 5. Energy-level diagram for the states of  $\text{SiF}_4$ ,  $\text{SiF}_4^+$ , and  $\text{SiF}_4^{+2}$ . The dashed lines represent a transition to the  $2p_{3/2}$  continuum of  $\text{SiF}_4^+$  and subsequent Auger decay to the two-hole states  $a-f$  of  $\text{SiF}_4^{+2}$  (see Fig. 4 for spectral correspondence). The solid lines represent a discrete transition to the  $2p^{-1}\sigma^*(a_1)$  excited state, which autoionizes to valence main lines  $[(\text{outer})^{-1}$  and  $(\text{inner})^{-1}]$  and satellites  $a'-f'$ . The valence orbitals are labeled generically as either inner- or outer-valence (see Table I for clarification). Some states and specific electron configurations have been omitted for clarity.

sponding Auger final states, we show in Fig. 5 an energy-level diagram depicting these states. The Auger final states  $a-f$  of  $\text{SiF}_4^{+2}$  are indicated generically, along with the parallel resonantly produced satellites  $a'-f'$ , in the notation of Fig. 4. There are two-hole states in both the  $\text{SiF}_4^+$  and  $\text{SiF}_4^{+2}$  manifolds, differing only by the presence of an excited  $\sigma^*(a_1)$  electron.

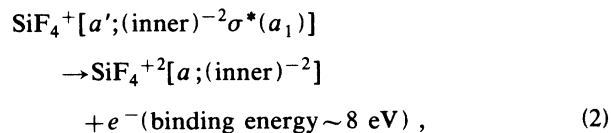
From Figs. 4 and 5, we see that some of the two-hole states are nearly degenerate with the single-hole inner-valence main lines ( $3t_2, 4a_1$ ) in  $\text{SiF}_4^+$ . This near degeneracy makes a straightforward distinction between inner-valence main lines and outer-valence satellites difficult, and probably indicates that configurational mixing is important in the inner-valence region. The spectrum of Aksela *et al.*<sup>17</sup> agrees with ours, except that they did not observe the highest-binding-energy satellite  $a'$ .

There is a kinetic energy shift between the resonant spectrum and the Si  $L_{2,3}VV$  Auger spectrum. We note that this shift is not readily apparent in Fig. 4, where the two spectra have been aligned to facilitate comparison. To first order, this shift might be expected to be equal to the difference between the resonance energy and the corresponding  $2p$  continuum, which is 5.5 eV for  $\text{SiF}_4$ . This is based on the simple picture that each resonance state  $a'-f'$  is made up of the corresponding Auger final state  $a-f$ , plus one electron in the resonant  $\sigma^*(a_1)$  orbital. The observed shift in our spectra varies from 8–10 eV for peaks  $a'-f'$ , slightly higher than the average shift of 7.5(5) eV reported by Aksela *et al.*<sup>17</sup> However, energy shifts from both sets of data contain variations from peak to peak and uncertainties of  $\pm 1$  eV in the absolute shift. The increased shift of 8–10 eV is easily understood as follows. The 5.5-eV shift between the  $2p^{-1}\sigma^*(a_1)$  state is

just the binding energy of an electron in the  $\sigma^*(a_1)$  orbital, starting from the  $\text{SiF}_4[2p^{-1}\sigma^*(a_1)]$  initial state:



For the analogous process of removing an electron from the excited  $\sigma^*(a_1)$  orbital in the  $a'$  state of  $\text{SiF}_4^+$ ,



the shift is naturally larger because of the attraction between the additional (positive) valence holes and the excited  $\sigma^*(a_1)$  electron.

The above comparison with the Auger spectrum illustrates that much of the resonant-state decay proceeds like above-threshold Si  $L_{2,3}VV$  Auger decay; the excited electron  $\sigma^*(a_1)$  remains as a spectator while one valence electron fills the Si  $2p$  hole and another is ejected. The resonant final states have the same two valence holes as the Auger features, but they also include the initially excited electron  $[\sigma^*(a_1)]$ . We note that the resonances below the Si  $2p$  threshold in  $\text{SiH}_4$  also decay to a number of spectator satellites, in analogy to the two-hole states in the Auger spectrum.<sup>28</sup>

We emphasize the qualitative and incomplete nature of this result for predominant spectator decay. It is probable that the initially excited electron gets “shaken up” to a higher unoccupied orbital or “shaken off” into the continuum in a substantial fraction of the decays. This is in analogy to atomic Xe  $4d \rightarrow 6p, 7p$  resonant decay, where shake-up to the next higher  $np$  level is significant,<sup>29</sup> and to atomic Ar, Kr, and Xe inner-shell resonances, where shake-off is an appreciable fraction of the resonant decay.<sup>30</sup> The energy separation of a spectator and a shake-up satellite configuration of  $\text{SiF}_4^+$  would differ by as little as 2 eV for the  $\sigma^*(a_1)$  resonance, making an exact orbital assignment for the loosely bound electron difficult. However, the overall similarity between the Auger and resonant spectra does appear to implicate spectator decay as an important decay mode.

To help quantify the extent of satellite decay, partial cross sections for the outer-valence main lines and for peaks  $e'$  and  $f'$  are shown in Fig. 6. For the summed outer-valence main lines we see a small enhancement of  $\sim 10\%$  at resonance. This is larger than the upper limit of 5% reported by Aksela *et al.*<sup>17</sup> Production of these main lines is a measure of the degree of participation of the excited electron in the resonant decay. For the inner-valence region, low count rates and limited resolution prohibited reliable partial cross-section measurements on each satellite peak listed in Table III. However, peaks  $e'$  and  $f'$  were sufficiently resolved, and their cross sections are also shown in Fig. 6. All the profiles mimic the total photoabsorption profile, indicating either very little interference between direct ionization and autoionization via the excited state, or that peaks  $e'$  and  $f'$  actu-

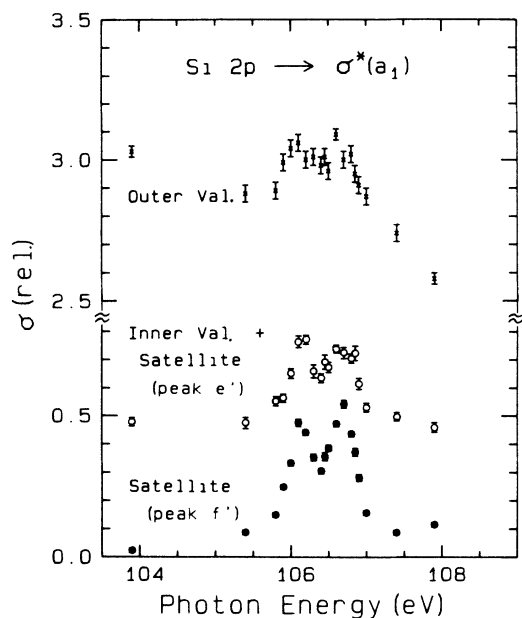


FIG. 6. For the  $\text{Si } 2p \rightarrow \sigma^*(a_1)$  discrete excitation, we show the relative partial cross sections for the outer-valence main lines ( $\times$ 's), inner-valence main lines, and possibly an overlapping satellite corresponding to peak  $e'$  in Fig. 4 (open circles), and the satellite peak  $f'$  from Fig. 4 (closed circles). The small effect ( $\sim 10\%$ ) on the outer-valence main lines is an indication of a small amount of participation of the initially excited electron in the decay process.

ally contain different final states on and off resonance.

We now estimate the overall relative amounts of satellite versus main-line decay. Though we do not have quantitative results for satellites  $a'-d'$ , we do observe that the relative intensities on resonance are roughly comparable to the analogous intensities in the Auger spectrum. Using this as a working hypothesis, we find that the ratio of the summed intensity in satellites  $a'-d'$  relative to satellite  $f'$  is (from Table II)  $\sim 1.3(1)$ , where the uncertainty reflects the differences between our results and those of Aksela *et al.*<sup>17</sup> This yields an intensity on the scale of Fig. 6 of 0.65(6) for the sum of peaks  $a'-d'$ .

The remaining uncertainty in an estimate of satellite versus main-line decay is related to the possible presence of a satellite in peak  $e'$  in addition to the inner-valence main lines. If the resonant-satellite spectrum carries relative intensities about equal to those in the Auger spectrum, then all of the enhancement in peak  $e'$  can be ascribed to a satellite, with very little effect on the inner-valence main lines. This assumption would suggest that  $\sim 80\%$  of the  $\sigma^*(a_1)$  resonant decay to  $\text{SiF}_4^+$  results in satellite production. A lower limit of 60% derives from the assumption of only main-line enhancement in peak  $e'$ .

This range of 60–80% for satellite decay within the  $\text{SiF}_4^+$  manifold may also indicate roughly the amount of spectator decay if the excited electron remains in the  $\sigma^*(a_1)$  orbital. We have already mentioned the possibility of shake-up to a higher orbital which can still result in a satellite final state. Higher spectral resolution and de-

tailed calculations would be required to differentiate between the spectator satellites and satellites involving shake-up to a higher level.

### B. Higher resonances—qualitative results

For the higher-energy resonances, we show two resonant spectra in Fig. 7, corresponding to  $h\nu=108.8$  and 110.6 eV, and a nonresonant spectrum at  $h\nu=107.9$  eV. These spectra were taken with a bandpass of 0.25 eV in an attempt to resolve the assigned  $\sigma^*(t_2)$  molecular-orbital excitation from the Rydberg excitations (see Fig. 1).

As with the  $\sigma^*(a_1)$  resonance, the outer-valence orbitals show no dramatic enhancement at the higher resonances. Figure 7 shows the inner-valence region only up to  $\sim 50$  eV binding energy, above which the peak intensities are extremely low. Aksela *et al.*<sup>17</sup> have obtained comparable spectra at  $h\nu=109$  and 111 eV extending out to 75 eV binding energy.

For our 108.8-eV spectrum, we see enhancement of the inner-valence main-line peak, and a satellite peak appears at lower binding energy [37(1) eV]. This satellite peak corresponds to peak  $F''$  in the Aksela *et al.*<sup>17</sup> spectrum and possibly to peak  $f$  in the Auger spectrum. The satellite configuration presumably would contain two valence holes and an excited  $\sigma^*(t_2)$  electron.

For our spectrum at  $h\nu=110.6$  eV in the vicinity of the 3d, 4d, and 5s Rydberg states, we observe enhancement of the inner-valence peak at 40 eV binding energy, and a satellite peak appears at 44(1) eV binding energy.

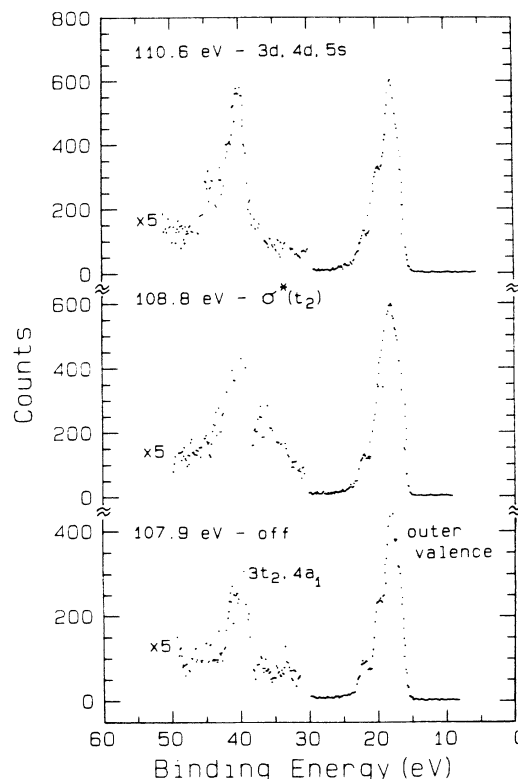


FIG. 7. Photoelectron spectra taken at the higher excitations at photon energies 110.6, 108.8, and off resonance at 107.9 eV. The monochromator bandpass was 0.25 eV.

This satellite is labeled as  $S_1$  in the Aksela *et al.*<sup>17</sup> spectrum, with no clear correspondence to a peak in the Auger spectrum.

The more extended energy-range results of Aksela *et al.*<sup>17</sup> suggest that the spectra at these higher resonances generally resemble the Auger spectrum, but with a few additional peaks. For example, the peaks labeled  $S_1$  (binding energy  $\sim 44$  eV) and  $S_{2,3}$  (binding energy  $\sim 35$  eV) appear in spectra at  $h\nu=109$  and  $111$  eV in addition to the inner-valence main lines and peaks  $c-f$ .<sup>17</sup> Overall, their interpretation is that a spectator-satellite spectrum results, shifted from the Auger spectrum.<sup>17</sup> We agree, but believe that these additional peaks add a complication that is not yet clearly understood.

Dirac-Fock calculations<sup>17</sup> on atomic Si confirm the positions of the Rydberg states in  $\text{SiF}_4$ , in agreement with a recent assignment<sup>9</sup> but contrary to an earlier interpretation which assigned all the features in the 108–111-eV range as Rydberg excitations.<sup>14</sup> One particularly convincing argument for the overlapping molecular-orbital (MO) and Rydberg assignment of Friedrich *et al.*<sup>9</sup> is the apparent quenching of the Rydberg excitations in solid  $\text{SiF}_4$ . Very recently, photoemission work on Si 1s excitation and ionization in gaseous  $\text{SiF}_4$  suggests that a third model involving distortion of the tetrahedral geometry to a trigonal bipyramid (TBP) leads to yet another interpretation of this absorption spectrum.<sup>16</sup> With the symmetry change in the excited state (due to the static Jahn-Teller effect<sup>31</sup>), the dipole selection rules are altered. These authors find the assumption of  $C_{2v}$  symmetry to be consistent with three dipole-allowed transitions to  $a_1^*$ ,  $b_1^*$ , and  $b_2^*$  orbitals, which can explain the resonances between  $h\nu=108$ – $112$  eV.<sup>16</sup> The assignment of  $\sigma^*(a_1)$  for the 106.1- and 106.7-eV resonances is retained. With this distorted excited state, the solid  $\text{SiF}_4$  results of Friedrich *et al.*<sup>9</sup> are explained by a  $C_{3v}$  geometry, in contrast to a  $C_{2v}$  geometry in the gas phase.

Based on our results, we find support for predominant decay to spectator satellites, but insufficient evidence to distinguish between the interpretations mentioned above (overlapping MO and Rydberg<sup>9</sup> versus distorted excited-state geometry<sup>16</sup>). The original MO and Rydberg model<sup>9</sup> explains the solid photoabsorption spectrum and is a natural extension of trends seen in the spectra of other Si- and S-containing molecules. There exist clearly understood examples where either MO or Rydberg transitions dominate the absorption spectrum (as with  $\text{SF}_6$  and  $\text{SO}_2$ , respectively<sup>1</sup>). It is thus possible to view  $\text{SiF}_4$  as an intermediate case, with comparable intensity in both localized (MO) and diffuse (Rydberg) states. However, there remains the problem of explaining the two intense resonances 5.7 and 4.3 eV below the Si 1s edge in  $\text{SiF}_4$ .<sup>16</sup> A recent redetermination<sup>32</sup> of the absolute energy scale for this Si 1s measurement<sup>16</sup> (a shift of 2.2 eV to higher energy) may also alter the distorted excited-state interpretation. Calculations on the distorted  $C_{2v}$  and  $C_{3v}$  excited states could indicate whether the energies of the proposed Si 2p and 1s excitations agree with the observed values, and help to resolve the assignment of the Si 2p discrete excitations investigated in this work.

## V. THE Si 2s EXCITATIONS

The total cross section (Fig. 1) shows a single broad feature near 160 eV related to discrete excitations of the Si 2s electron. To interpret the specific transitions involved we can make use of the Si 1s excitation spectrum<sup>16</sup> because the Si 1s and 2s initial states both have  $a_1$  symmetry. As noted in Sec. IV B, the Si 1s discrete spectrum is not consistent with the expected dipole-allowed transition to a  $t_2^*$  orbital, but rather shows two strong resonances. Bodeur *et al.*<sup>16</sup> have proposed an explanation for both the Si 1s and 2s spectra by invoking a trigonal bipyramid excited-state geometry. These authors propose that the doublet seen below the Si 1s edge corresponds to excitation into axial and equatorial orbitals of the TBP geometry. By analogy, a Coster-Kronig decay step ( $L_1L_{2,3}V$ -type) could broaden a doublet for the Si 2s resonant feature near 160 eV to the observed single peak.

We have studied the resonant decay channels in the vicinity of the Si 2s excitations. Our cross-section results in Fig. 3 show no measurable resonant effect in either the Si 2p or valence main lines near 160 eV. We note that Auger peak  $d$  overlaps in this energy region with the Si 2p main line. This Auger intensity was subtracted as a correction to the Si 2p main-line cross section, increasing the intensity error to  $\pm 10\%$  for the cross section.

The only other accessible decay channels lead to Si 2p shake-up satellites and resonant shake-off (which is not easily visible in our spectra). We show spectra taken near the peak of the Si 2s resonance (159.9 eV) and below the resonance (156.9 eV) in Fig. 8. These spectra qualitatively illustrate the enhancement of Si 2p satellites which

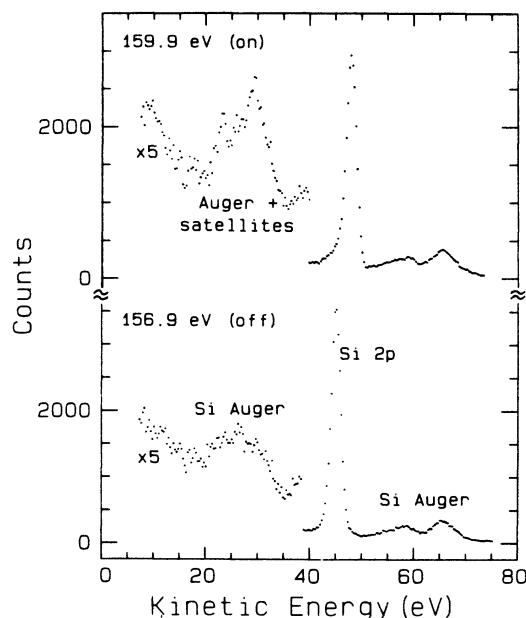


FIG. 8. Photoelectron spectra taken in the vicinity of the Si 2s excitations near  $h\nu=160$  eV. The nonresonant spectrum (bottom panel) illustrates the presence of the Si Auger peaks between 20 and 35 eV kinetic energy. On resonance (top panel), the peak structure in this region changes, suggesting enhancement of Si 2p satellites.

overlap with part of the Si  $L_{2,3}VV$  Auger spectrum (peaks *a* and *b*). The binding energies of these satellites are 130–140 eV, with an excitation energy relative to main-line ionization of 20–30 eV.

The branching ratio for these peaks (Auger peaks *a* and *b* plus satellites) relative to the Si 2*p* main line is presented in Fig. 9. The nonresonant value for this ratio is ~15% in agreement with an expected 14% based on the relative intensities of peaks *a* and *b* in the Auger spectrum (see Table II). Because the Si Auger intensity should track the Si 2*p* main-line intensity, a change in the ratio in Fig. 9 indicates only satellite enhancement. The (satellite)/(Si 2*p*) intensity ratio on resonance is then 13(2)%, which accounts for about half of the resonant intensity in the total photoabsorption curve (see Fig. 1). In addition to a possible small effect (within our  $\pm 10\%$  error) in the Si 2*p* main-line cross section, the remaining intensity could appear as decay to other satellites or shake-off channels.

At least half of the decay of the excited state(s) thus occurs via an  $L_1L_{2,3}V$  step producing an ion with a Si 2*p* core hole and a valence hole plus an electron in a loosely bound orbital, likely to be the initially excited orbital. This fast Coster-Kronig-type decay helps to explain the width of the absorption feature. We have no experimental evidence to indicate the specific transition(s) taking place near  $h\nu=160$  eV. The eventual assignment of the more easily distinguished Si 1*s* discrete transitions should help to clarify similar processes for Si 2*s* excitation.

## VI. CONCLUSIONS

For the Si 2*p* continuum of SiF<sub>4</sub>, our photoemission results confirm photoabsorption measurements which detected two intense resonances at  $h\nu=117$  and 133 eV. At the first resonance, the Si 2*p* partial cross section exhibits a pronounced effect consistent with photoabsorption but disagrees with a much smaller enhancement observed by Bancroft *et al.*<sup>13</sup> No enhancement at either resonance was found for the valence main lines or satellites, in contrast to a resonant satellite at the  $e_g$  shape resonance in the S 2*p* continuum of SF<sub>6</sub>.<sup>8</sup> The one-electron model for describing shape resonances<sup>1,5</sup> thus qualitatively applies to these Si 2*p* resonances which decay only to the Si 2*p* main line.

We have interpreted the Si  $L_{2,3}VV$  Auger spectrum by invoking a variation in the extent of hole-hole interactions from one final-state configuration to another. In this approach, the molecular orbitals used to calculate hole-interaction energies are, of course, delocalized. This model is an extension of the interpretation of Rye and Houston,<sup>18</sup> which assumes two valence holes localized in the same or different spatially distinct Si—F bonds. However, we still view the assignment of the Si  $L_{2,3}VV$  Auger spectrum as unresolved in light of preliminary calculations<sup>27</sup> which indicate that even a treatment of hole-

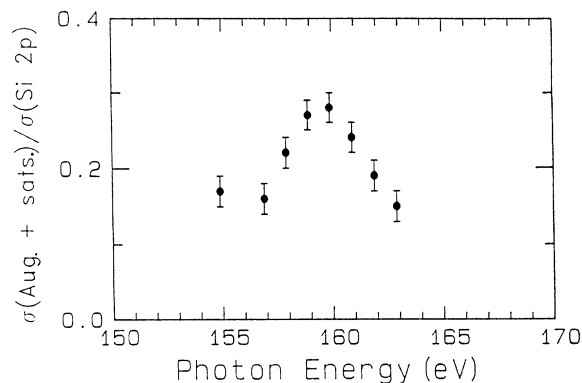


FIG. 9. Intensity ratio of the summed Auger and satellite peaks shown in Fig. 7 relative to the Si 2*p* main line. The ratio profile is in qualitative agreement with the total photoabsorption cross section (Ref. 9).

hole interaction energies does not fully explain all the major Auger peaks.

For the discrete resonances below the Si 2*p* edge and in particular for the  $\sigma^*(a_1)$  excitation, spectator decay to valence satellites is found to be a dominant decay mode. The satellite configurations thus parallel those for the Auger final states. In addition, configurational mixing of some of these satellites nearly degenerate with the inner-valence main lines is probably important.

The overall assignment of the discrete resonances in SiF<sub>4</sub> is still in question, with the exception of the  $\sigma^*(a_1)$  resonance. In light of new photoabsorption results on the Si 1*s* core-level ionization,<sup>16,32</sup> the possibility of a distorted excited state may change the point group symmetry and thus the classification of the molecular-orbital excitations. This interpretation, as applied to the Si 2*p* and 1*s* discrete resonant features, does not include any appreciable intensity in Rydberg transitions, in contrast to the model of Friedrich *et al.*<sup>9</sup> Theoretical calculations are needed which examine the role of the static Jahn-Teller effect for neutral molecules with a core hole and an excited electron. This would help sort out the relative contribution of molecular-orbital and Rydberg states below the core-level thresholds of SiF<sub>4</sub>.

## ACKNOWLEDGMENTS

We thank I. Nenner for sending copies of Refs. 16, 28, and 32 prior to publication and F. P. Larkins and G. M. Bancroft for helpful discussions. This work was supported by the Director, Office of Energy Research, Office of Basic Energy Sciences, Chemical Sciences Division of the U.S. Department of Energy under Contract No. DE-AC03-76SF00098. It was performed at the Stanford Synchrotron Radiation Laboratory, which is supported by the U.S. Department of Energy's Office of Basic Energy Sciences.

- \*Present address: National Bureau of Standards, Gaithersburg, MD 20899.
- †Permanent address: Department of Chemical Sciences and Technologies, University of Rome II, via Orazio Raimondo, 00173 Rome, Italy.
- ‡Present address: Technische Universität München, Physik-Department (E20), D-8046 Garching bei München, Federal Republic of Germany.
- <sup>1</sup>J. L. Dehmer, *J. Chem. Phys.* **56**, 4496 (1972), and references therein.
- <sup>2</sup>A. A. Pavlychev, A. S. Vinogradov, T. M. Zimkina, D. E. Onopko, and S. A. Titov, *Opt. Spektrosk.* **47**, 73 (1979) [*Opt. Spectrosc. (USSR)* **47**, 40 (1979)].
- <sup>3</sup>A. A. Pavlychev, A. S. Vinogradov, and T. M. Zimkina, *Opt. Spektrosk.* **52**, 231 (1982) [*Opt. Spectrosc. (USSR)* **52**, 139 (1982)].
- <sup>4</sup>M. Ya. Amusya, A. A. Pavlychev, A. S. Vinogradov, D. E. Onopko, and S. A. Titov, *Opt. Spektrosk.* **53**, 157 (1982) [*Opt. Spectrosc. (USSR)* **53**, 91 (1982)].
- <sup>5</sup>J. L. Dehmer, in *Resonances in Electron-Molecule Scattering, van der Waals Complexes, and Reactive Chemical Dynamics*, edited by D. G. Truhlar (American Chemical Society, Washington, D.C., 1984); J. L. Dehmer, D. Dill, and A. C. Parr, in *Photophysics and Photochemistry in the Vacuum Ultraviolet*, edited by S. P. McGlynn, G. Findley, and R. Huebner (Reidel, Dordrecht, 1985); J. L. Dehmer, A. C. Parr, and S. H. Southworth, in *Handbook on Synchrotron Radiation*, edited by G. V. Marr (North Holland, Amsterdam, 1986), Vol. II.
- <sup>6</sup>T. M. Zimkina and V. A. Formichev, *Dokl. Akad. Nauk SSSR* **169**, 1304 (1966) [*Sov. Phys.—Dokl.* **11**, 726 (1967)].
- <sup>7</sup>T. M. Zimkina and A. S. Vinogradov, *J. Phys (Paris)* **32**, C4-3 (1971).
- <sup>8</sup>T. A. Ferrett, D. W. Lindle, P. A. Heimann, M. N. Piancastelli, P. H. Kobrin, H. G. Kerkhoff, U. Becker, W. D. Brewer, and D. A. Shirley, *J. Chem. Phys.* (to be published).
- <sup>9</sup>H. Friedrich, B. Pittel, P. Rabe, W. H. E. Schwarz, and B. Sonntag, *J. Phys. B* **13**, 25 (1980).
- <sup>10</sup>B. W. Yates, K. H. Tan, G. M. Bancroft, L. L. Coatsworth, and J. S. Tse, *J. Chem. Phys.* **83**, 4906 (1985).
- <sup>11</sup>M. M. Gofman, V. A. Andreev, and V. I. Nefadov, *J. Electron Spectrosc.* **37**, 375 (1986).
- <sup>12</sup>P. R. Keller, J. W. Taylor, F. A. Grimm, P. Senn, T. A. Carlson, and M. O. Krause, *Chem. Phys.* **74**, 247 (1983).
- <sup>13</sup>G. M. Bancroft, S. Aksela, H. Aksela, K. H. Tan, B. W. Yates, L. L. Coatsworth, and J. S. Tse, *J. Chem. Phys.* **84**, 5 (1986).
- <sup>14</sup>W. Hayes and F. C. Brown, *Phys. Rev. A* **6**, 21 (1972).
- <sup>15</sup>M. B. Robin, *Chem. Phys. Lett.* **31**, 140 (1975).
- <sup>16</sup>S. Bodeur, I. Nenner, and P. Millie (private communication).
- <sup>17</sup>S. Aksela, K. H. Tan, H. Aksela, and G. M. Bancroft, *Phys. Rev. A* **33**, 258 (1986).
- <sup>18</sup>R. R. Rye and J. E. Houston, *J. Chem. Phys.* **78**, 4321 (1983).
- <sup>19</sup>M. G. White, R. A. Rosenberg, G. Gabor, E. D. Poliakoff, G. Thornton, S. Southworth, and D. A. Shirley, *Rev. Sci. Instrum.* **50**, 1288 (1979).
- <sup>20</sup>S. Southworth, C. M. Truesdale, P. H. Kobrin, D. W. Lindle, W. D. Brewer, and D. A. Shirley, *J. Chem. Phys.* **76**, 143 (1982).
- <sup>21</sup>S. Southworth, U. Becker, C. M. Truesdale, P. H. Kobrin, D. W. Lindle, S. Owaki, and D. A. Shirley, *Phys. Rev. A* **28**, 261 (1983).
- <sup>22</sup>C. N. Yang, *Phys. Rev.* **74**, 764 (1948).
- <sup>23</sup>F. Wuilleumier and M. O. Krause, *J. Electron Spectrosc.* **15**, 15 (1979).
- <sup>24</sup>D. W. Lindle, T. A. Ferrett, P. A. Heimann, and D. A. Shirley, *Phys. Rev. A* **34**, 1131 (1986).
- <sup>25</sup>T. A. Carlson, W. A. Svensson, M. O. Krause, T. A. Whitley, F. A. Grimm, G. Von Wald, J. W. Taylor, and B. P. Pullen, *J. Chem. Phys.* **84**, 122 (1985).
- <sup>26</sup>F. P. Larkins, *J. Chem. Phys.* **86**, 3239 (1987).
- <sup>27</sup>F. P. Larkins (private communication).
- <sup>28</sup>G. G. B. de Souza, P. Morin, and I. Nenner, *Phys. Rev. A* **34**, 4770 (1986).
- <sup>29</sup>V. Schmidt, S. Krummacher, F. Wuilleumier, and P. Dhez, *Phys. Rev. A* **24**, 1803 (1981).
- <sup>30</sup>P. A. Heimann, D. W. Lindle, T. A. Ferrett, S. H. Liu, L. J. Medhurst, M. N. Piancastelli, D. A. Shirley, U. Becker, H. G. Kerkhoff, B. Langer, D. Szostak, and R. Wehlitz, *J. Phys. B* **20**, 5005 (1987).
- <sup>31</sup>J. H. D. Eland, *Photoelectron Spectroscopy* (Halsted, New York, 1974).
- <sup>32</sup>S. Bodeur, I. Nenner, and P. Millie (private communication).
- <sup>33</sup>G. Biery, L. Åsbrink, and W. Von Niessen, *J. Electron Spectrosc.* **27**, 129 (1982).
- <sup>34</sup>W. B. Perry and W. L. Jolly, *J. Electron Spectrosc.* **4**, 219 (1974).